



**CUSTOM HEAT RELEASE RATE TESTING OF AN
ELECTRIC VEHICLE LITHIUM ION BATTERY**

FINAL REPORT
Consisting of 28 Pages

SwRI® Project No.: 01.19142.01.001
Test Date: March 13, 2013
Report Date: May 3, 2013

Prepared for:

Exponent, Inc.
17000 Science Drive, Suite 200
Bowie, MD 20715

Prepared by:

K.C.

Karen C. Carpenter, M.S.
Research Engineer
Fire Resistance Section

Approved by:

For:
Barry L. Badders, M.E., P.E.
Manager
Fire Resistance Section

This report is for the information of the client. This report shall not be reproduced except in full, without the written approval of SwRI. Neither this report nor the name of the Institute shall be used in publicity or advertising.



1.0 INTRODUCTION

The objective of this test program was to perform a custom fire test to measure the heat release rate (HRR) and burning behavior of an *Electric Vehicle Lithium Ion Battery*, when subjected to a propane fueled fire, for Exponent, Inc., located in Bowie, MD. Additionally, the products of combustion were sampled and analyzed using Fourier Transform Infrared (FTIR) spectroscopy for various gases. Testing was conducted March 13, 2013, at Southwest Research Institute's (SwRI) Fire Technology Department, located in San Antonio, Texas.

This test methodology is intended to measure and describe the properties of materials or products in response to heat and flame under controlled laboratory conditions. The results should not be used alone to describe or appraise the fire hazard or the fire risk of materials, products, or assemblies under actual fire conditions. However, results of this test may be used as elements of a complete fire hazard assessment or a fire risk assessment, which takes into account all the factors that are pertinent to an assessment of the fire hazard or fire risk of a particular end-use. The results apply specifically to the specimens tested, in the manner tested, and not to similar materials, nor to the performance when used in combination with other materials.

2.0 DESCRIPTION OF TEST SPECIMEN

An *Electric Vehicle Lithium Ion Battery* was received by SwRI on January 16, 2013. The battery was "T" shaped with an overall length of 64 in. and a width of 33¾ in. at the cross member. The height of the battery varied from 11½–12¾ in. and a 2¼-in. lip was present around the bottom of the battery along the entire perimeter. The battery can be seen in Figure 1. The battery was provided at a 100% state of charge and weighed approximately 400 lb.



Figure 1. *Electric Vehicle Lithium Ion Battery.*

Additionally, Exponent, Inc., provided a rack to hold the battery during testing, four 19-in. diameter circular propane burners, gas train equipment, and a data acquisition system capable of recording the gas flow and internal battery information.

3.0 EXPERIMENTAL SETUP

3.1. Setup

The test rack was constructed under SwRI's 20 × 20-ft calorimetry exhaust hood, which is instrumented to measure heat release and smoke production. Gypsum wallboard was placed under the test rack to protect the laboratory floor from heat during testing. The propane burners were supported using concrete blocks which resulted in the burners being located 14 in. from the floor and 6 in. below the bottom of the battery. The four burners were arranged in a "T" layout to provide equal flame exposure to the bottom of the battery. Figure 2 shows the burners lit, in place, prior to placing the battery over them.



Figure 2. Propane Burners Setup Prior to Testing.

A 10 × 10-ft truncated cone steel hood was centrally located over the test setup. This setup was chosen in order to concentrate the products of combustion for FTIR analysis, as significant dilution would occur if sampling was conducted in the exhaust duct of the 20 × 20-ft hood. The hood was open at the top to allow the products of combustion to be drawn through the smaller hood and into the 20 × 20-ft calorimetry hood. A gas sampling tube provided with nine 1-mm holes was located across the opening in the top of the 10 × 10-ft hood and was connected to a heated sample transfer line. A pump drew the gases through the sample transfer line and was used to fill the Tedlar grab bags. This setup is shown in Figure 3.



Figure 3. Gas Sampling Hood and Large Calorimetry Hood.

Additional pictures of the test setup can be found in Appendix A. See Appendix B for detailed drawings of the test set up.

3.2. Instrumentation

A total of 16 Type K thermocouples (TCs) were located in and around the battery in order to measure temperatures throughout the test. TCs 1–12 were affixed to the exterior surface of the battery using Omegabond CC High Temperature Bonding cement. The cement was located over the TC bead and allowed to dry for at least 24 hr prior to testing. TC's 13–15 were located inside of the three vents on the battery. The TC was placed such that the bead was located 1 in. below the vent opening. After placement of the TC inside the battery, the vent was covered using the Client-provided self-adhesive covers. In addition to the vent covers, foil tape was used to hold the TC in place. TC 16 was located approximately 1 in. under the bottom surface of the battery to measure the temperature of the burner flames.

Four 0–50-kW/m² Schmidt-Boelter heat flux gauges were used during testing. Two of the heat flux gauges were located 5 ft from the edge of the battery and the remaining two were located 10 ft from the battery edge. A Type K TC was located next to each heat flux gauge.

During testing, the HRR was measured using the oxygen consumption technique. This technique requires the measurement of gas concentrations in the exhaust duct, as well as the volumetric flow of these gases. The products of combustion and entrained air were collected in a hood and extracted through an exhaust duct by a fan. A gas sample are drawn from the exhaust duct and analyzed for oxygen, carbon dioxide, and carbon monoxide concentrations. The gas temperature and differential pressure across a

bi-directional probe were measured for calculating the mass flow rate of the exhaust gases. The smoke production and temperature measurements were also taken throughout the duration of the test.

Digital photographs were taken before, during, and after the test. During testing, digital video was taken. The test video is provided on DVD.

3.3. Test Methodology

The data acquisition systems were started and a 2-min baseline was taken. The propane burners were then ignited and the visual timer started. The propane flow rate was adjusted during the first 2–3 min of the test. The propane burners were turned off 20 min into the test and the battery was allowed to burn until it self-extinguished at 1 hr 34 min.

4.0 TEST RESULTS

Testing was conducted March 13, 2013, at SwRI's Fire Technology Department. A summary of the test results is provided in Table 2. Because this testing was conducted to assess the burning characteristics of the setup and not to a standard test method, there are no acceptance criteria and no judgment as to pass or failure can be made. Detailed drawings of the test set up and instrumentation layout are included in Appendix B. Appendix C includes detailed observations and test results, including graphs.

4.1. Heat Release Results

During the first 20 min of the test, some of the products of combustion were not captured by the large calorimetry hood. This resulted in measured HRR values that were lower than the actual values. In an effort to better estimate the actual HRR, the Point Source Radiation model (see NFPA Handbook, 10th Edition, p. 3-156) was utilized. This model can be used to calculate the HRR, based on the heat flux measurements. A value of 0.35 was used for the radiative fraction and is an average of the SFPE Handbook values for propane and the nylon exterior of the battery. Additionally, the radial distance used was based on the distance between the center of the battery and the heat flux gauge. The point source model has a bias factor of 2.02 (NUREG-1934, Nuclear Power Plant Fire Modeling Analysis Guidelines) and a standard deviation of 0.59. This was taken into account in the final calculations shown in the summary table and the HRR graph.

In addition to calculating the heat release based on oxygen consumption and heat flux, the heat release was calculated using CO₂ generation. The results of all three calculations are included in Appendix C. In an attempt to more accurately calculate the HRR based on heat flux, the results were compared with the HRR using oxygen consumption and CO₂ generation during the non-peak heat release periods when theoretically, all the HRR values should be the same as all the smoke was being captured by the calorimetry hood. The point source HRR was approximately 30% lower than the other HRR measurements during these periods. Therefore, a second point source HRR line was graphed using values 30% higher than calculated using the model and factoring in the bias factor.

At various times during the test, a “jet” of flame was visible in one direction. For example, at 20 min 58 s, there was a 3–4 ft flame shooting horizontally from the harness area directly towards the East heat flux gauge as shown in Figure 4. This results in a high heat flux during that period and consequently a high HRR calculated using the point source model.



Figure 4. Test at 20 min 58 s.

The data acquisition system used to measure the TCs and heat flux gauges dropped several data points between 36 min 10 s and 37 min 54 s. These points did not occur near any peaks and have been omitted from the graphs.

4.2. Toxicity Results

A total of 14 air samples were taken using the Tedlar grab bags. Sampling was conducting every 5 min starting at 5 min into the test. Each sample was pulled over a 1-min period. The bags were then analyzed for HCl, HF, HBr, HCN, CO₂, CO, NO_x, SO₂, acrolein, and formaldehyde using SwRI’s Thermo Fischer Nicolet 6700 FTIR. The results were reviewed and showed only CO and CO₂ present. Each spectra was directly examined for the vapor phase signatures for HCN and none were detected which means that other signals are causing a false positive interferent, usually water vapor. Additionally, each spectra was examined for HF. No HF was detected; however, it is noted that a noisy baseline resulted in some false-positive readings. Results of the CO and CO₂ measurements are graphed along with the measurements taken in the calorimetry hood using a Servomex analyzer. The variance in results shows the dilution that occurs when the sample is taken from the large hood versus sampling right above the product. Detailed results are included in tabular form in Appendix C

Table 2. Summary of Test Results.

O₂	Depletion	Maximum HRR _{total}	698 kW	at	17 min 33 s
		Average HRR _{total}	128 kW		
		Total Heat Released	720 MJ		
CO₂	Generation	Maximum HRR _{total}	684 kW	at	17 min 43 s
		Average HRR _{total}	152 kW		
		Total Heat Released	857 MJ		
Point Source	Calculation	Maximum HRR _{point source}	860 kW	at	14 min 52 s
		Average HRR _{point source}	146 kW		
		Total Heat Released	824 MJ		
Peak Radiant Heat Flux		Maximum Smoke Release Rate	5.70 m ² /s	at	4 min 8 s
		Average Smoke Release Rate	1.00 m ² /s		
		Total Smoke Released	5664 m ²		
		Maximum Optical Density	0.55 1/m	at	4 min 8 s
		Maximum Duct Flow Rate	4.51 m ³ /s		
		Average Optical Density	0.104 1/m		
		Average Volumetric Duct Flow Rate	3.92 m ³ /s		
		East Heat Flux (5')	17.1 kW/m ²	at	21 min 40 s
		North Heat Flux (10')	4.7 kW/m ²	at	15 min 50 s
		South Heat Flux (5')	18.0 kW/m ²	at	14 min 52 s
West Heat Flux (10')		3.7 kW/m ²	at	14 min 52 s	

APPENDIX A
PHOTOGRAPHS
(CONSISTING OF 8 PAGES)



Figure A-1. Test Setup (Viewed from East).



Figure A-2. Test Setup (Viewed from West).



Figure A-3. Close Up of Battery prior to Testing (Viewed from North).



Figure A-4. Test at 3 min 38 s.



Figure A-5. Test at 4 min 50 s.



Figure A-6. Test at 13 min 27 s.



Figure A-7. Test at 20 min 32 s.



Figure A-8. Test at 26 min 08 s.



Figure A-9. Test at 43 min 06 s.



Figure A-10. Test at 1 hr 1 min 32 s.



Figure A-11. Test at 1 hr 33 min 0 s.



Figure A-12. Post Test View of Battery (Immediately Post Test).



Figure A-13. Post-Test View of Battery.



Figure A-14. Post-Test View of Battery.



Figure A-15. Post-Test View of Battery (Dissected).



Figure A-16. Post-Test View of Battery (Dissected).

APPENDIX B
DRAWINGS OF TEST SETUP
(CONSISTING OF 2 PAGES)

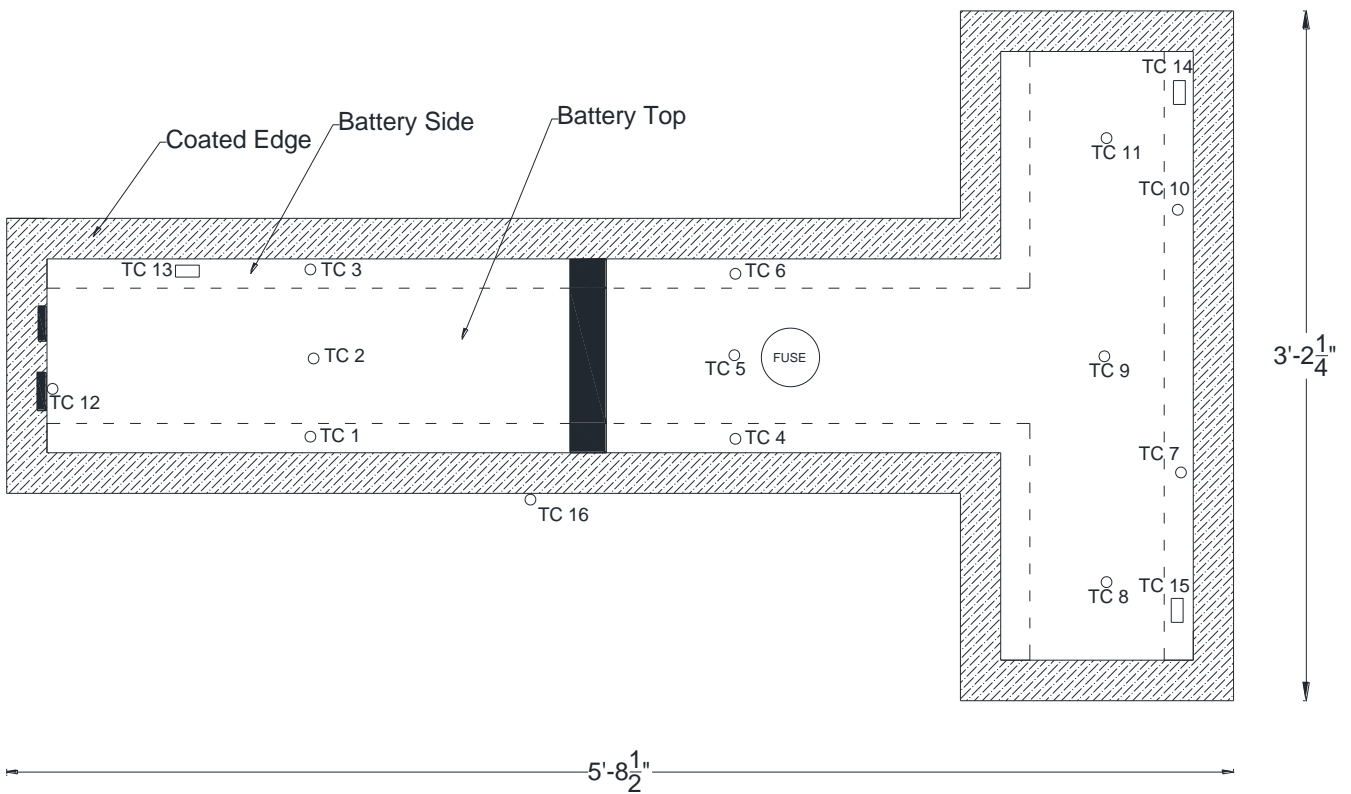


Figure B-1. Battery with TC Layout.

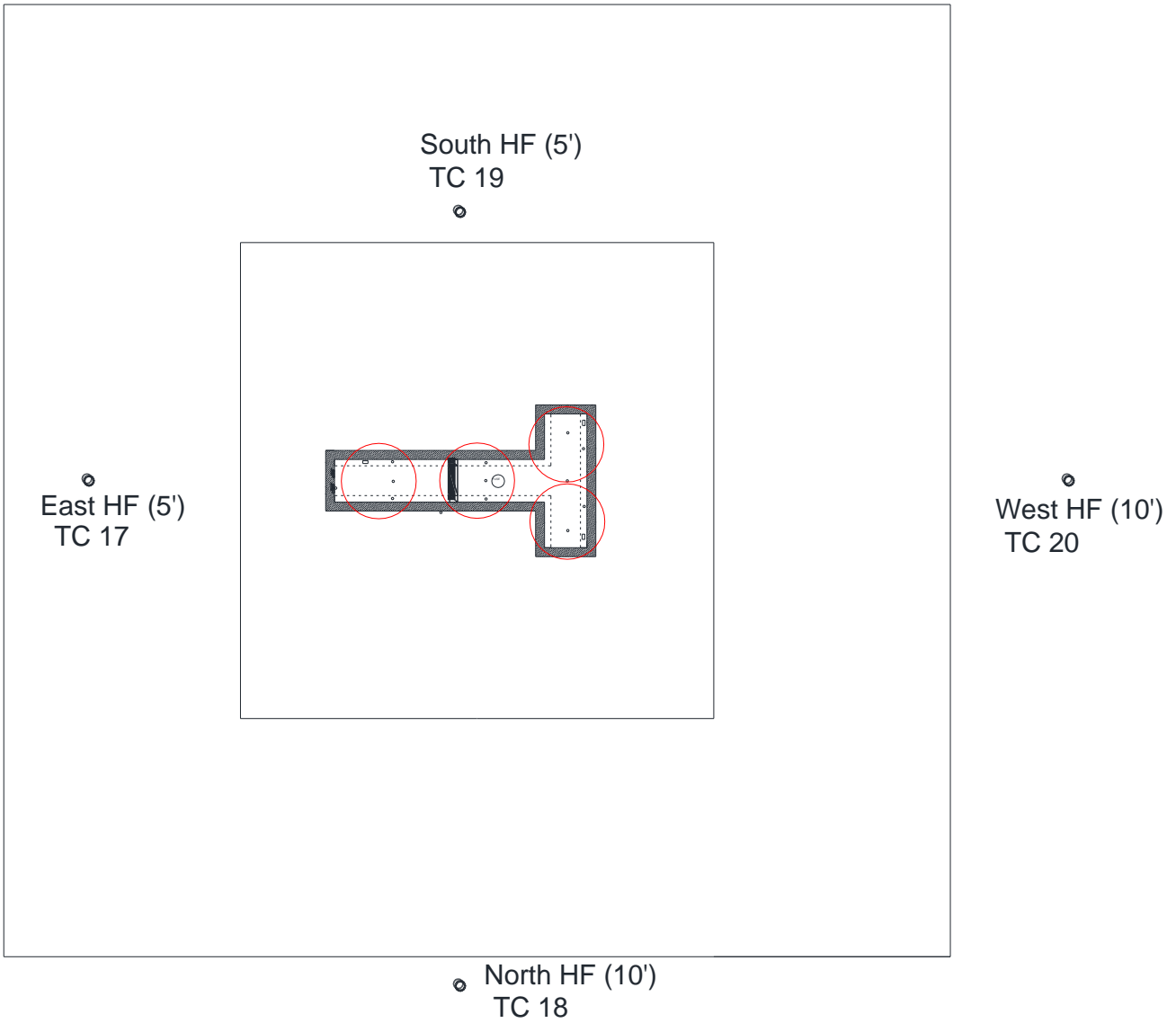
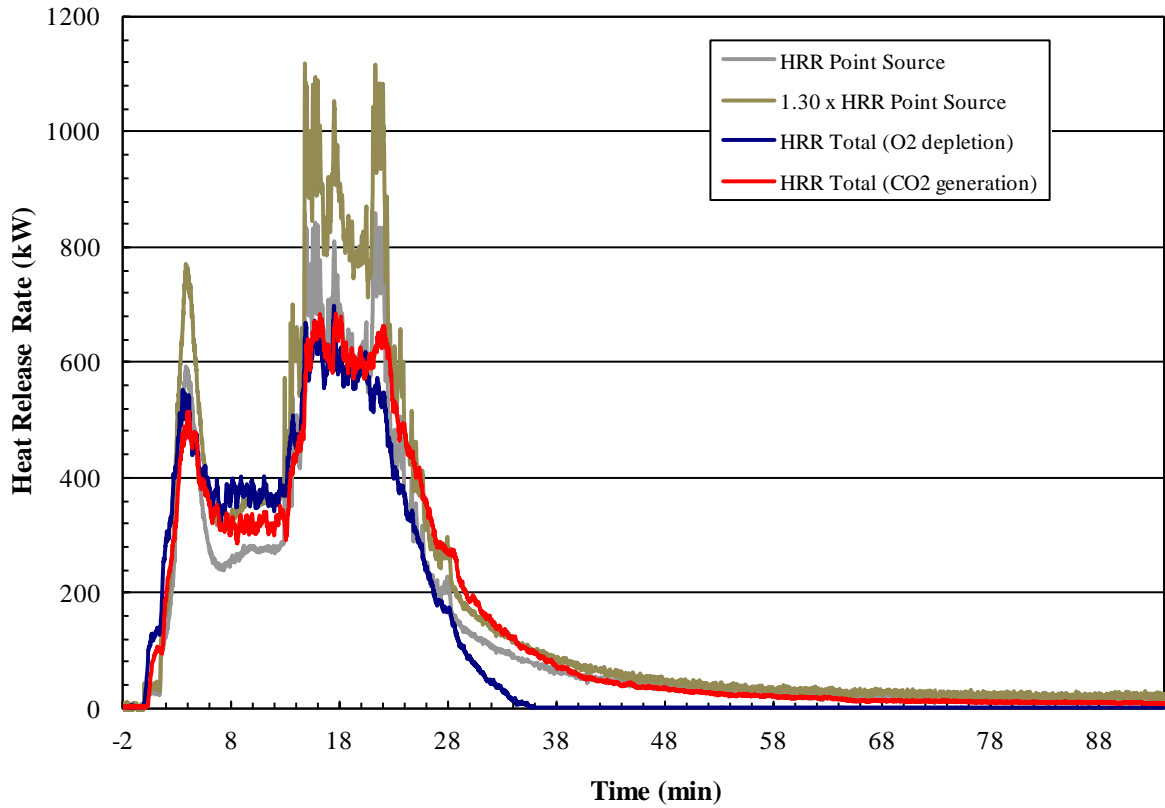


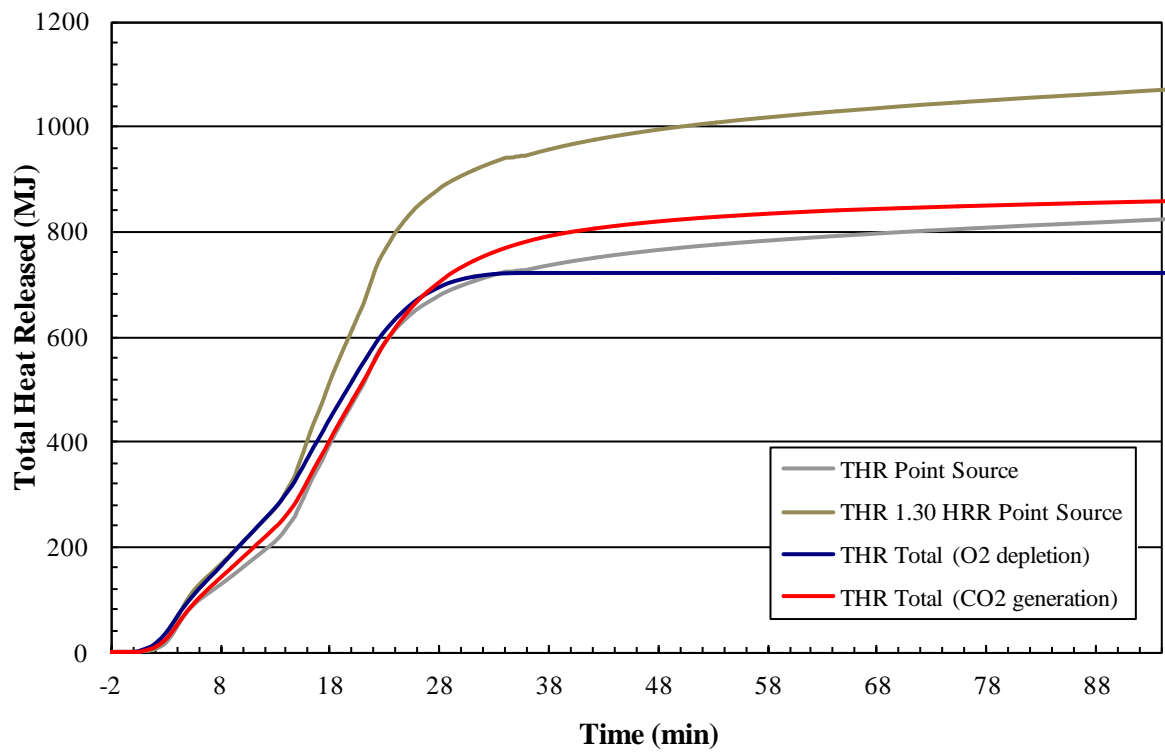
Figure B-2. Test Setup with Heat Flux Layout (Top View).

APPENDIX C
TEST DATA AND OBSERVATIONS
(CONSISTING OF 8 PAGES)

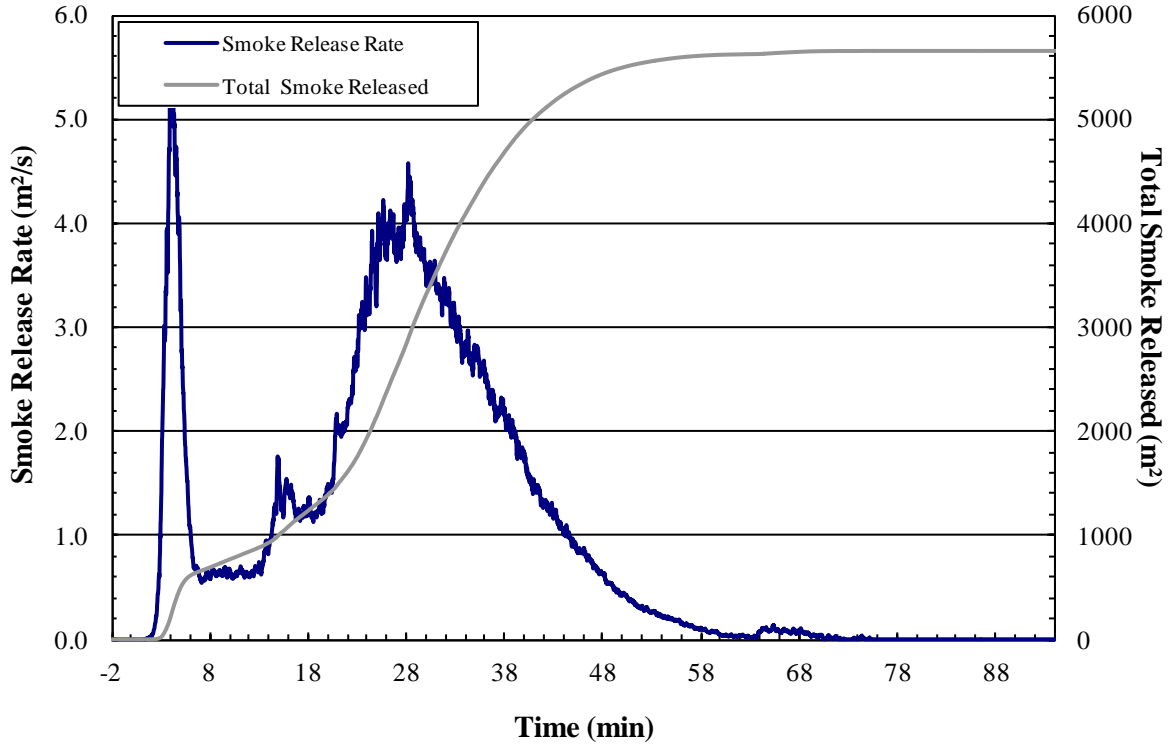
HEAT RELEASE RATE



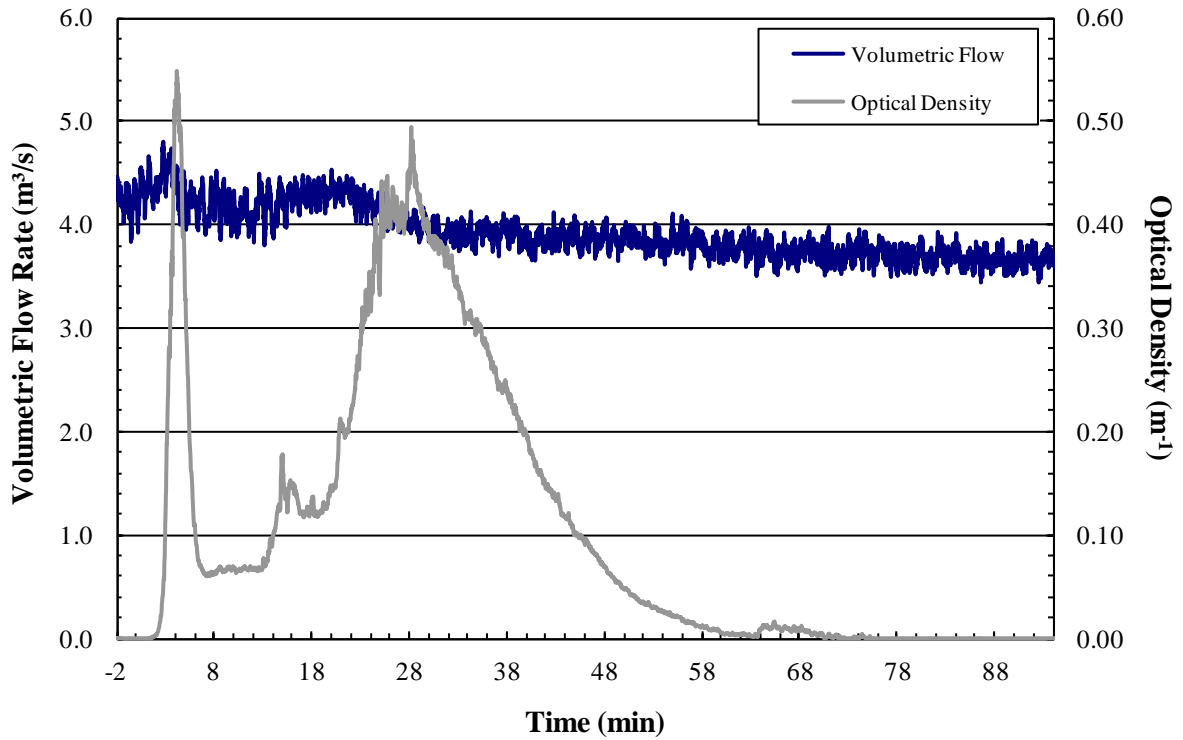
TOTAL HEAT RELEASED



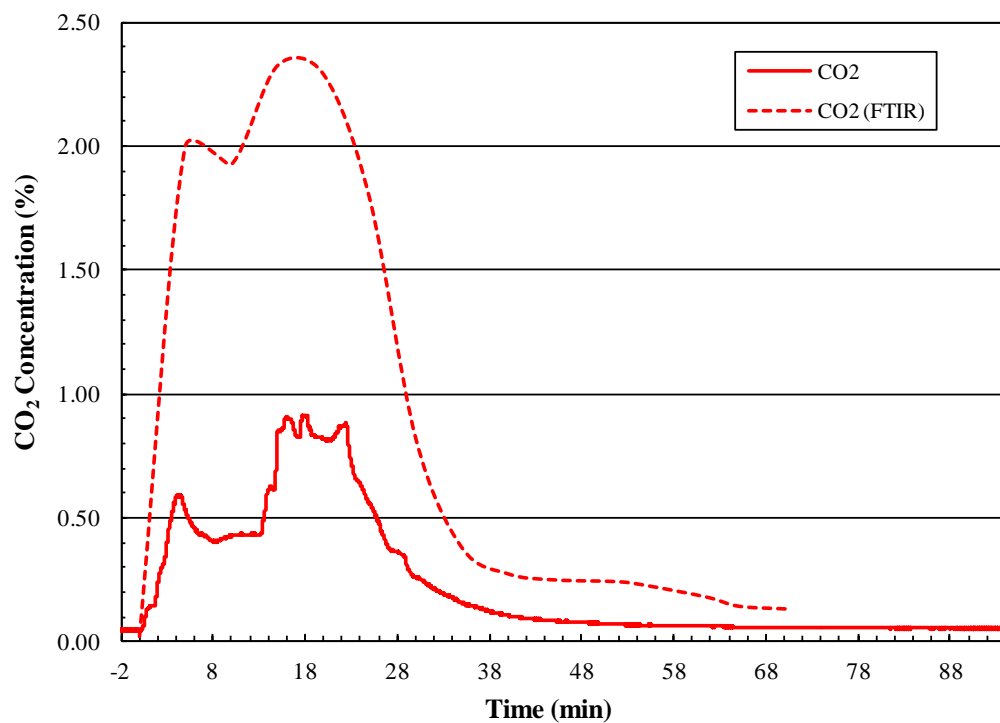
SMOKE RELEASE RATE AND TOTAL SMOKE RELEASED



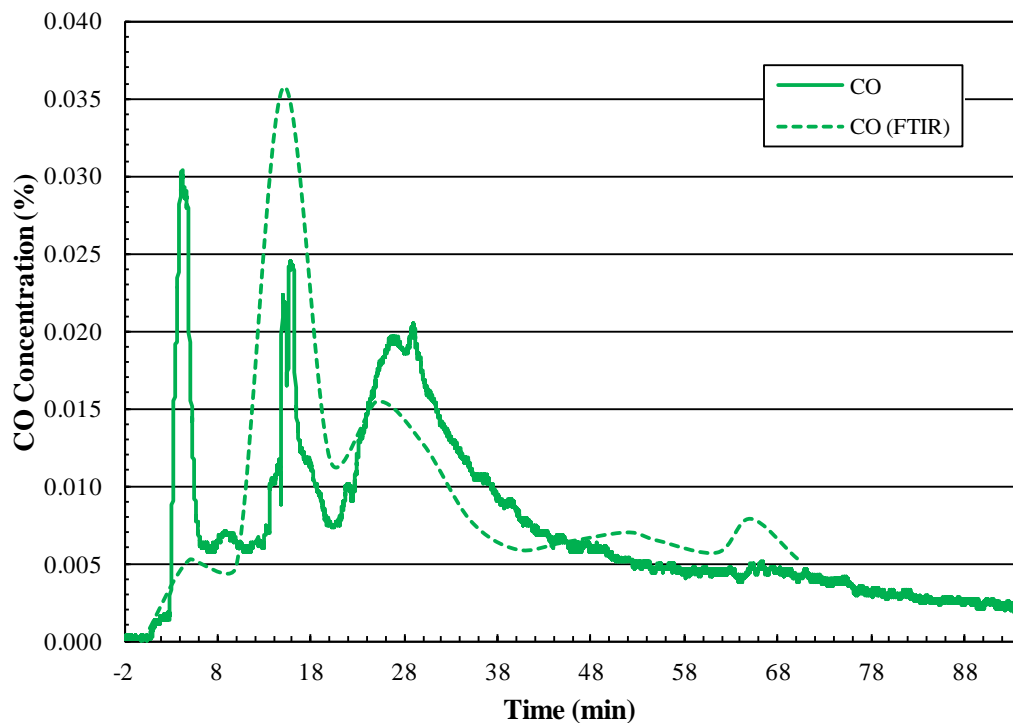
VOLUMETRIC DUCT FLOW RATE AND OPTICAL DENSITY



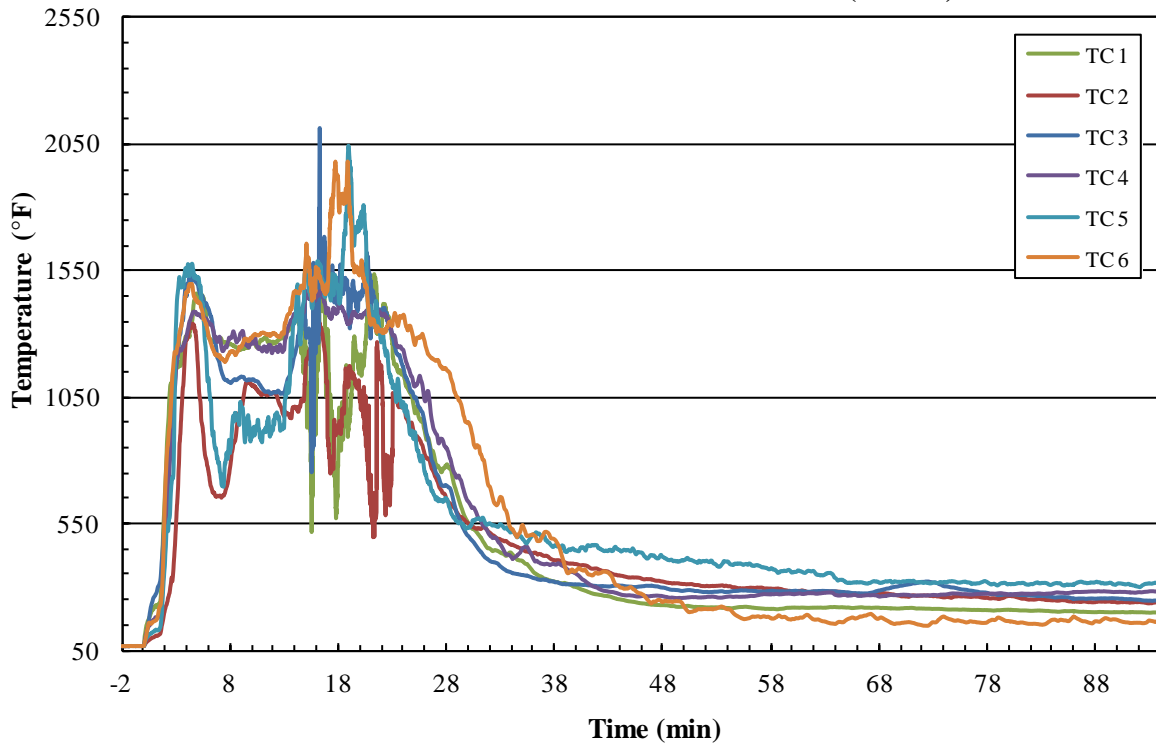
CO₂ Concentrations (Analyzer and FTIR)



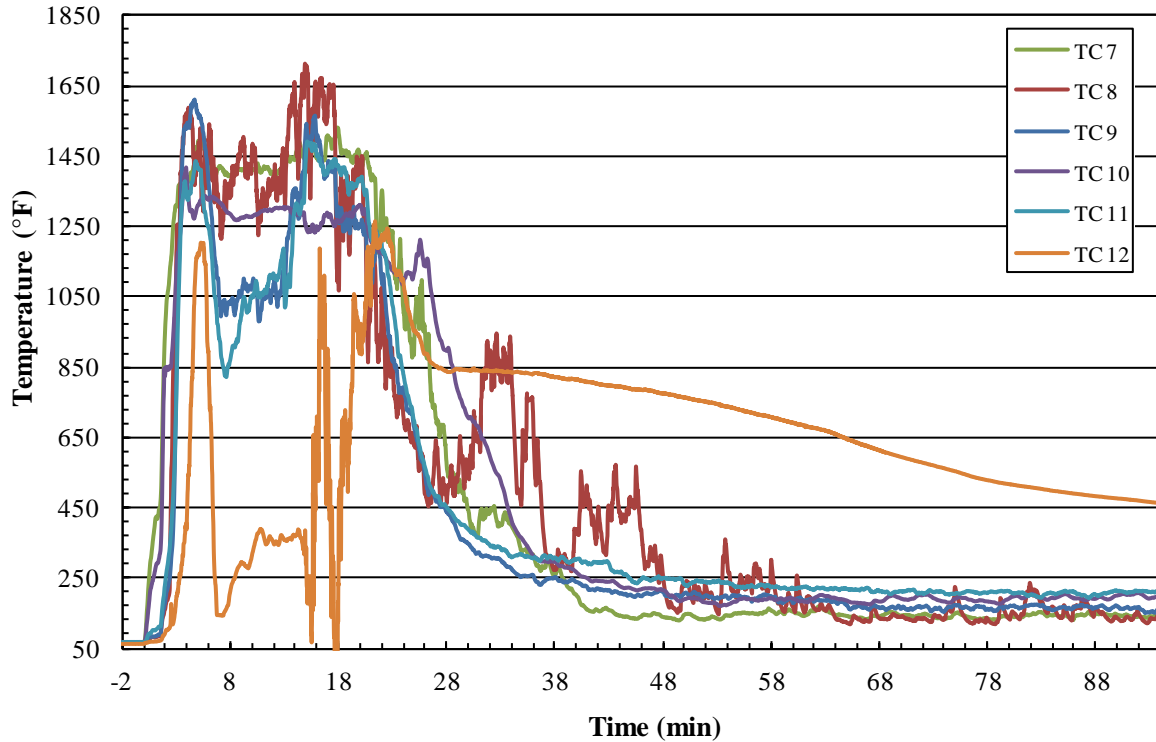
CO Concentration (Analyzer and FTIR)



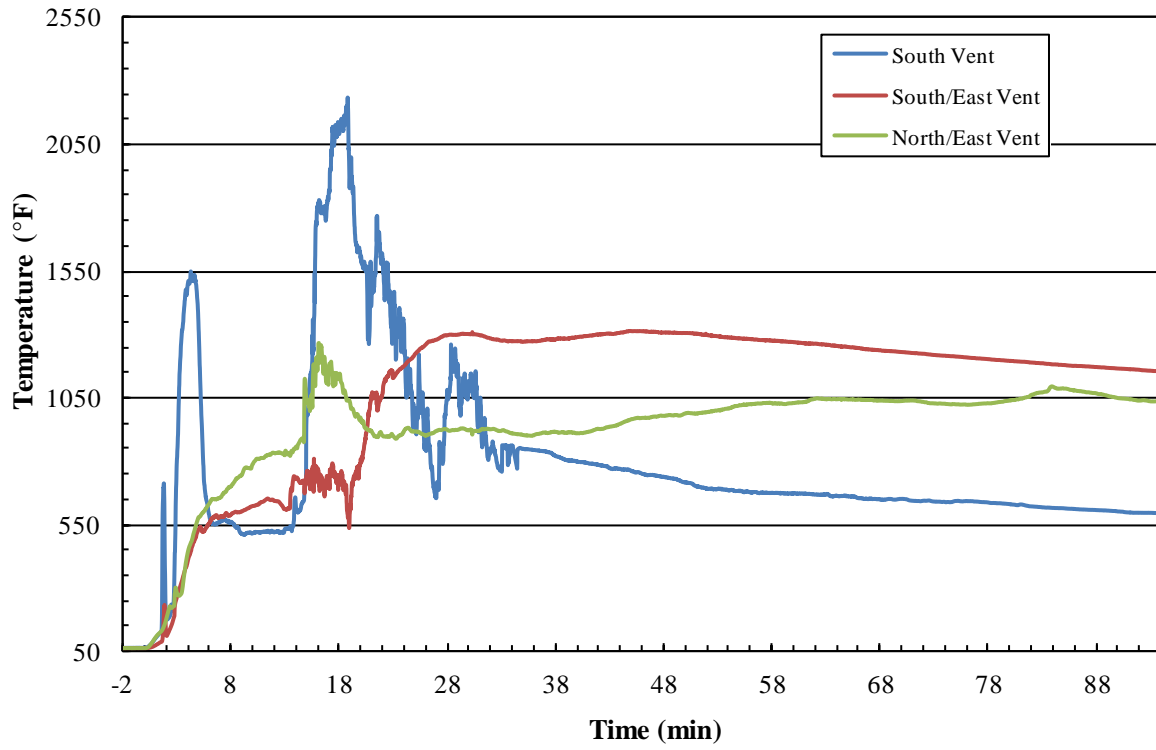
TEMPERATURES ON BATTERY SURFACE (TC 1-6)



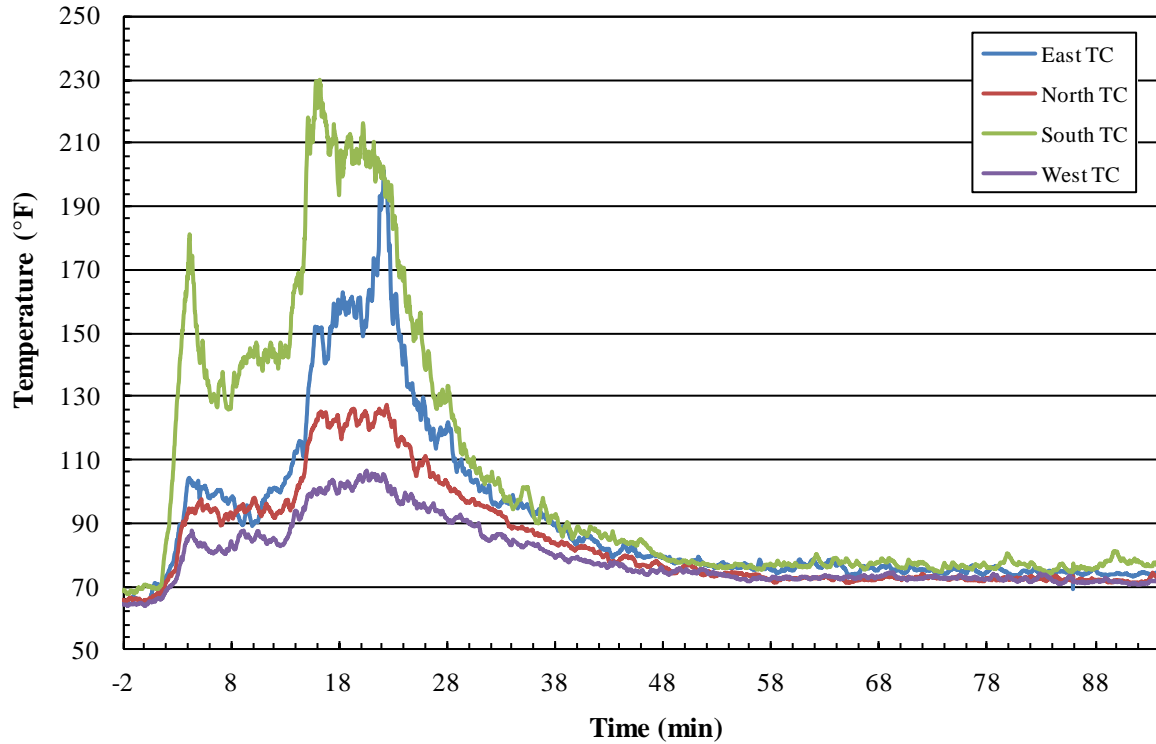
TEMPERATURES ON BATTERY SURFACE (TC 7-12)



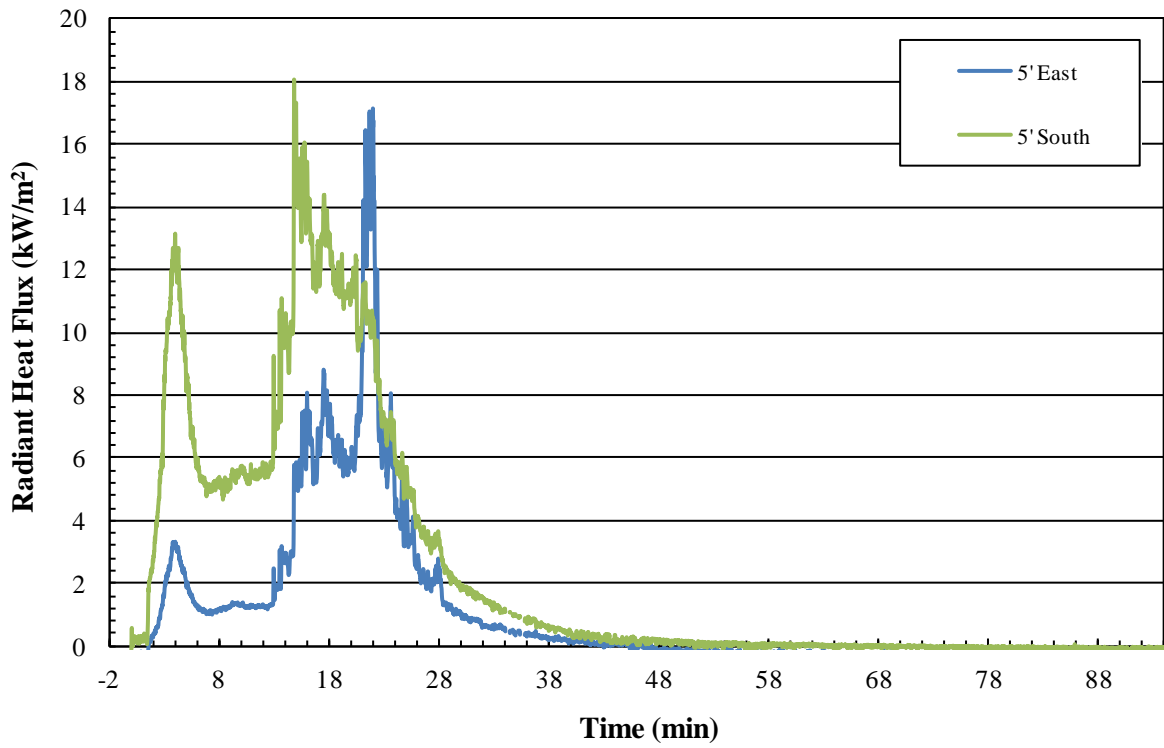
TEMPERATURES INSIDE BATTERY VENTS



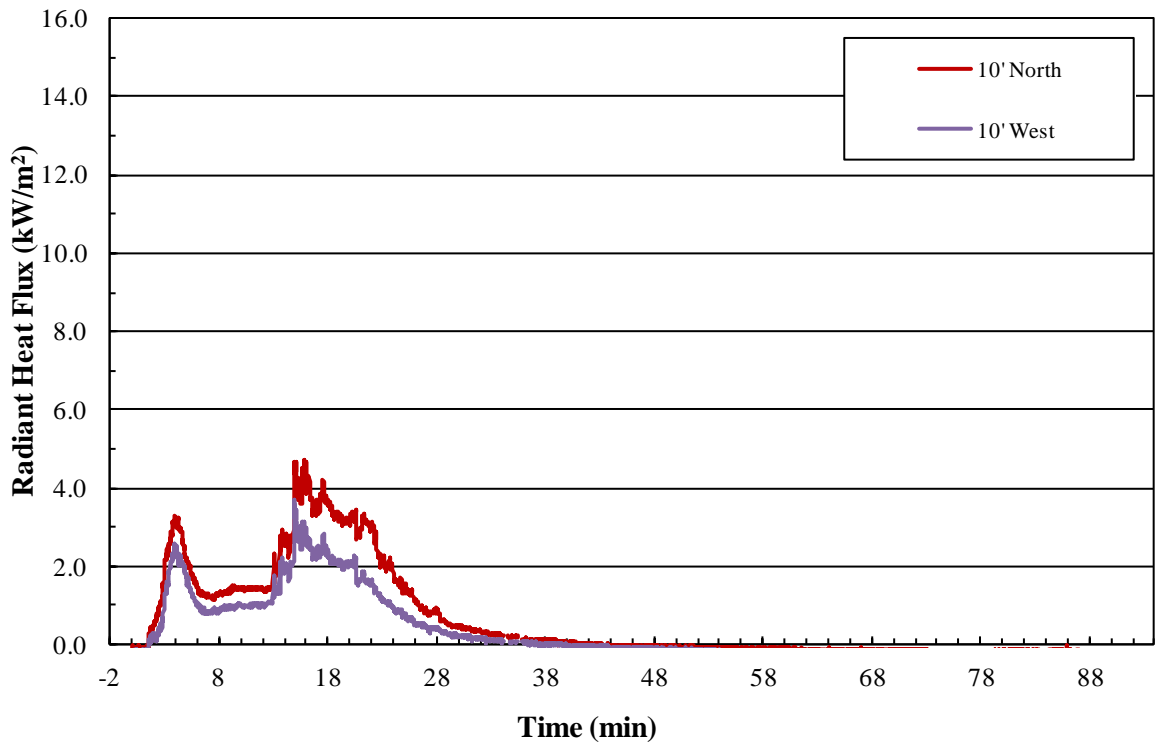
TEMPERATURES AT HEAT FLUX GAUGES



RADIANT HEAT FLUX-5 FT LOCATIONS



RADIANT HEAT FLUX-10 FT LOCATIONS



POINT SOURCE HEAT RELEASE RATE

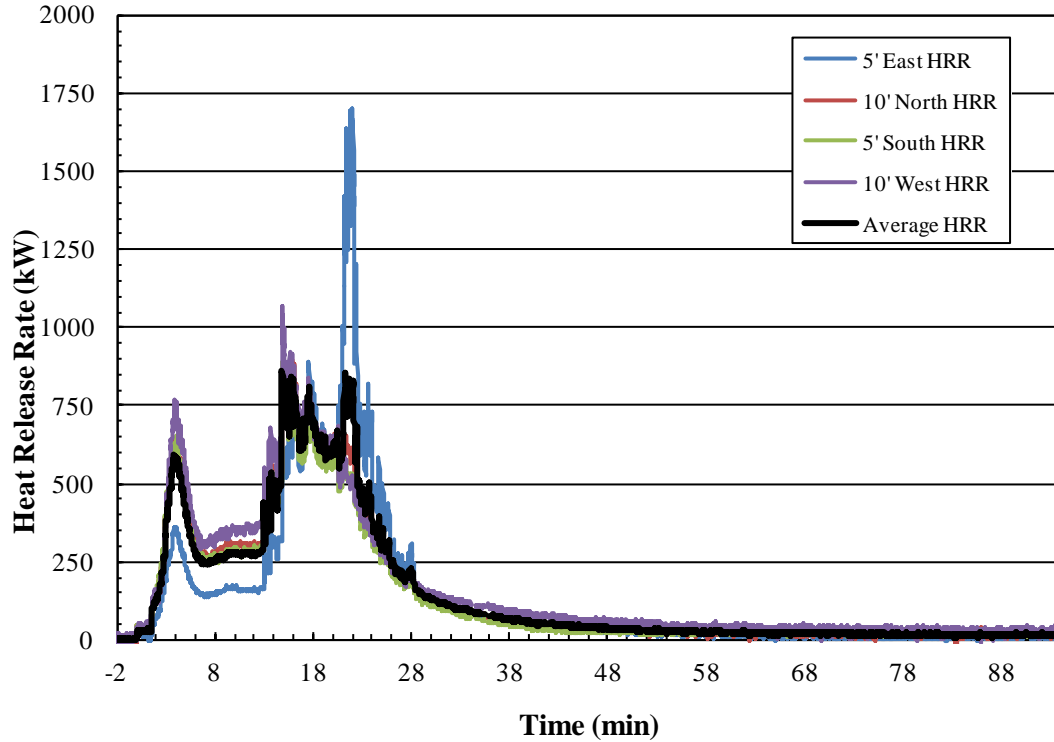


Table C-1. Visual Observations.

Time (hr:min:s)	Observations
-02:00	Baseline data collection begins.
00:00	Propane burners ignited (14-s delay for all burners to fully ignite).
00:46	Plastic coating on the battery edge ignites.
01:26	Propane flow adjusted.
02:16	Surface of battery is burning. Foil material peeling away.
02:40	Loud pop from battery.
09:50	Flames shooting 6–10 in. from the South battery vent.
12:00	10–12 in. flames from the top fuse.
20:21	Propane burners turned off.
47:10	Burning only near West battery vents, fuse harness area, and bottom edge.
49:00	South/West battery vent is smoking only.
1:03:00	A loud pop and the fire near the harness extinguishes.
1:04:00	Only remaining fire is in the North/West vent.
01:30:00	Popping noises coming from near the harness end.
01:34:00	Last remaining flamelet extinguishes. Battery continues to smoke. End of Test.

Table C-2. Results of FTIR Analysis.

Time (min)	CO	(+)CO	CO ₂	(+)CO ₂	HCN*	(+)HCN	SO ₂	(+)SO ₂	NO ₂	(+)NO ₂	HCL	(+)HCL	NO	(+)NO	HBr	(+)HBr	HF*	(+)HF
5	52.38	46.89	19938.75	6288.27	20.61	10.63	9.38	107.60	97.11	1021.36	-2.44	8.43	278.47	455.48	22.72	37.27	11.46	14.95
10	48.57	49.30	19240.94	5892.39	24.70	11.59	10.87	114.51	118.09	1104.97	2.87	8.92	295.98	487.46	25.25	41.37	12.99	15.00
15	356.72	72.46	23218.86	10539.18	31.99	15.27	-32.58	140.46	172.13	1451.01	-28.87	46.95	366.93	607.13	32.05	56.26	15.93	17.57
20	116.98	51.97	22870.66	9804.25	23.30	12.02	-2.68	115.48	156.44	1151.18	9.39	12.15	308.20	499.58	28.13	49.22	25.02	15.60
25	154.30	42.19	17859.01	5666.38	23.83	9.30	1.31	94.53	106.29	883.32	-2.79	12.93	237.47	396.92	23.65	40.25	23.66	13.66
30	126.72	40.32	8189.60	3458.22	26.67	8.64	1.30	90.48	86.98	847.58	4.22	13.39	224.26	379.32	21.81	36.21	7.66	13.58
35	77.81	37.74	3795.69	1058.06	23.68	8.76	0.92	91.82	82.90	857.09	2.86	14.16	220.68	383.74	22.25	37.44	10.37	15.86
40	58.85	38.18	2746.98	395.72	21.21	8.97	0.16	91.07	81.40	833.22	-1.73	12.93	214.59	376.62	20.63	30.08	4.07	12.87
45	63.38	36.30	2504.07	381.27	18.89	8.56	1.49	88.93	77.45	808.47	0.17	12.36	213.60	367.18	21.75	33.22	17.66	12.59
51.75	69.88	34.79	2433.94	370.77	18.69	8.87	0.00	88.63	82.11	830.80	3.04	13.54	215.77	369.24	15.44	25.42	19.33	13.31
55	64.72	34.88	2276.24	368.76	20.22	8.73	-0.17	87.79	82.32	813.41	6.74	12.44	213.82	364.37	17.46	25.29	17.84	13.11
61.5	56.96	32.88	1811.51	355.80	15.62	7.71	0.85	86.05	75.74	783.75	3.57	11.11	196.45	350.43	13.77	20.38	4.64	12.46
65	78.66	33.19	1442.41	330.74	19.75	8.06	-1.95	83.13	73.04	764.04	5.42	14.35	201.55	345.40	15.55	25.15	17.13	12.04
70	53.08	33.89	1335.05	332.35	18.66	8.27	-2.21	86.26	74.61	776.38	-4.73	12.08	207.08	354.05	16.86	27.84	18.19	12.06

(+) = Uncertainty

* All spectra were examined for all other gases. Only CO and CO₂ were detected. The values shown for HCN and HF are not real.